Material anisotropy in Wire and Arc Additively Manufactured structures

Ben Weber

WAAM in the construction industry

Additive manufacturing has found widespread research interest and industrial applications over the past decades. However, the construction industry is only starting to explore the benefits of this promising technology, mainly due to a lack of design guidelines that provide the necessary quality assurance procedures and standardise the manufacturing process [1,2,3]. Wire and Arc Additive Manufacturing (WAAM) is a metal 3D printing technique where an industrial robotic arm is used in conjunction with a conventional welding unit to deposit metal and create objects, with few limitations to their size or shape (Fig 1) [4].

Compared to other additive manufacturing methods, WAAM is especially interesting for the construction industry due to its high deposition rate (4-9 kg/h [5]) and the inherent surface tension of the molten metal which allows for overhanging structures to be printed without the need for support material [5]. Topologically optimised structures made possible by the digitally enabled manufacturing process, can exhibit the same structural strength but with considerably reduced material compared to conventional manufacturing techniques, which reduces the weight of the printed part and also its cost owing to the shorter manufacturing time [6]. These benefits also present interesting opportunities for the aerospace construction sector, which could allow for the production of large structural metal parts in space or other planetary bodies [7].

In contrast with conventionally produced stainless-steel structures, which behave in an isotropic way, those produced by WAAM can present considerable anisotropy [8,9,10]. Owing to the production process, where the crystallographic structure of the metal orientates itself relative to the distinct thermal gradient of the different layers during solidification, the mechanical behaviour of a structure is dependent on the printing direction relative to the loading direction [11]. An additional factor contributing to the anisotropic material behaviour is the surface finish of printed structures; surface undulations lead to a nonhomogeneous cross-sectional area, further increasing the directional dependency of the material [11]. Mainly owing to a scarcity of testing data [12], this anisotropic material behaviour is currently not fully understood, and no design and reliability recommendations can be given [5].

Material analysis

Prior work on analysing the material behaviour of Grade 308LSi stainless-steel WAAM [11] has determined that thin-walled stainless-steel WAAM can best be characterised as a planar orthotropic material. Proof and yield stresses as well as Young's moduli of the printed material have been derived for different printing directions, thicknesses and surface finishes. However, to accurately model the complete planar orthotropic behaviour and be able to simulate the material in finite element analysis (FEA), additional material characteristics, such as the Poisson's ratios and plastic behaviour, are needed.

This thesis uses the data of tensile tests from 37 as-built coupons (undulating surface from production still present) and 12 machined coupons (undulating surface removed using an end-mill, see Fig 2) to determine the missing material characteristics. The coupons were cut from larger plates at three different angles (0°, 45° and 90°) to the printing orientation to determine the material characteristics in these directions (see Fig 3) and at 2 different thicknesses for the as-built coupons (3.5 mm and 8.0 mm). Surface strain fields of the coupons during testing were determined via digital image correlation (DIC) which allowed, in addition to the longitudinal and transverse strains, for thickness strain measurements, which are very difficult to accurately determine with traditional methods. From the

stress-strain curves produced by these tests, a clearly anisotropic behaviour can immediately be detected (Fig 4). All three test orientations (0°, 45° and 90°) exhibit a distinctly different behaviour.

Elastic material behaviour

Elastic Poisson's ratios are determined from longitudinal and transverse surface strains in the elastic range. Fig 5 shows the individual Poisson's ratios derived from each machined coupon test as well as a numerically optimised model fitting the experimental data to a theoretical planar orthotropic material model. It can clearly be seen that the individual tests follow the expected model very closely. Fig 5 additionally shows how the Young's and shear moduli change over different off-axis loading angles. The elastic material constants derived from the tests: Young's moduli E, Poisson's ratios v and shear moduli G, see Table 1, show an anisotropic material behaviour of the WAAM structures and correlate well between the different material thicknesses and surface finishes. The variations in the material characteristics between the different coupon types was attributed to the varying influence of surface undulations depending on the coupon's thickness and surface finish. It is shown that the influence of the surface undulations becomes less important in thicker cross sections and approaches the material characteristics of machined structures.

Table 1: Material parameters WAAM [14]

	Machined coupons			As-built 3.5 mm			As-built 8.0 mm		
θ (°)	E_x (GPa)	ν_{xy} ()	G_{xy} (GPa)	E_x (GPa)	ν_{xy} ()	G_{xy} (GPa)	E_x (GPa)	ν_{xy} ()	G_{xy} (GPa)
0	143.7	0.419	100.9	137.4	0.458	98.1	142.8	0.443	95.0
45	219.5	0.088	50.1	188.5	-0.039	41.0	196.3	0.033	44.9
90	139.2	0.406	100.9	96.0	0.320	98.1	110.4	0.343	95.0

Plastic material behaviour

To accurately model the plastic material behaviour, the standard unidirectional yield model needs to be expanded to adapt to different material orientations. Plastic yield ratios (R-values), which can be determined from yield stresses using the Hill's yield criterion, are used. Their effect can be seen in the change of shape from the widely used von Mises yield surface (for isotropic materials) to the Hill's yield surface, see Fig 6. These yield stress ratios are used in FE to change the shape of the unidirectional material yielding curve at the different orientations.

The research from this thesis was used as a basis for the publication of two papers exploring the anisotropic material response of additively manufactured stainless steel using WAAM [13,14].

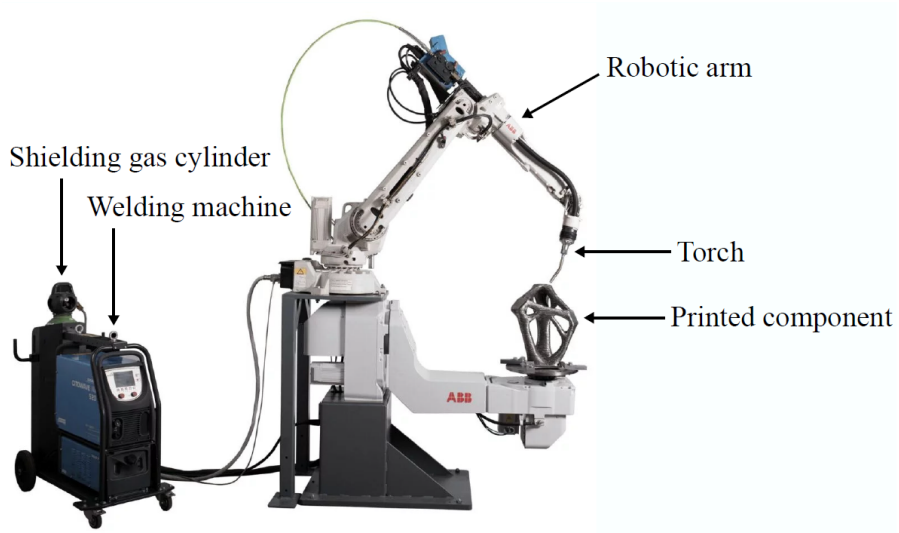

Fig 1: WAAM system [14]

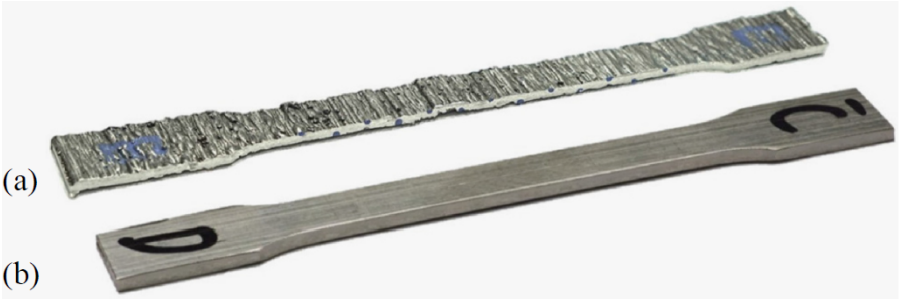

Fig 2: (a) As-built coupon and (b) Machined coupon [11]

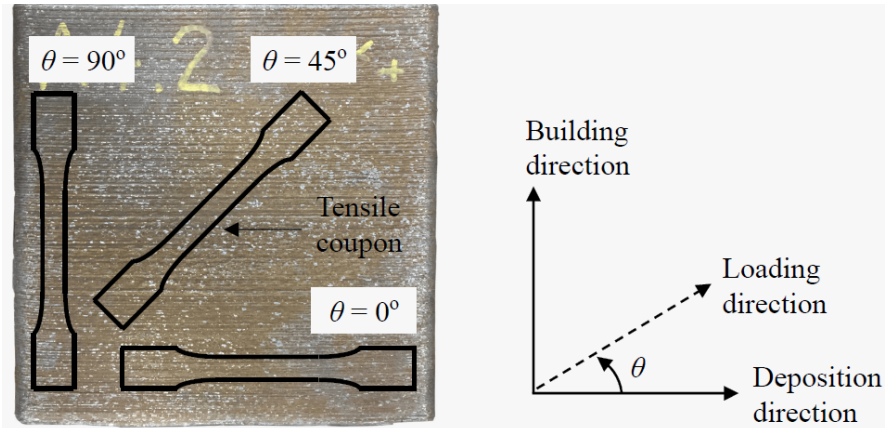

Fig 3: Coupon orientation relative to the deposition and building direction [14]

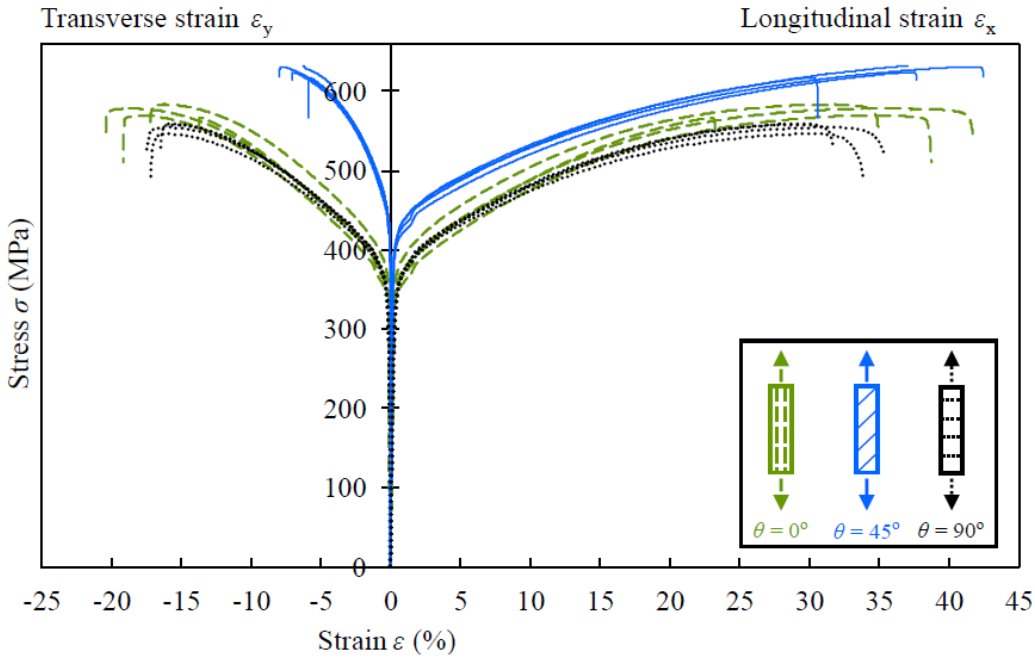

Fig 4: Stress–strain responses of the machined specimens [14]

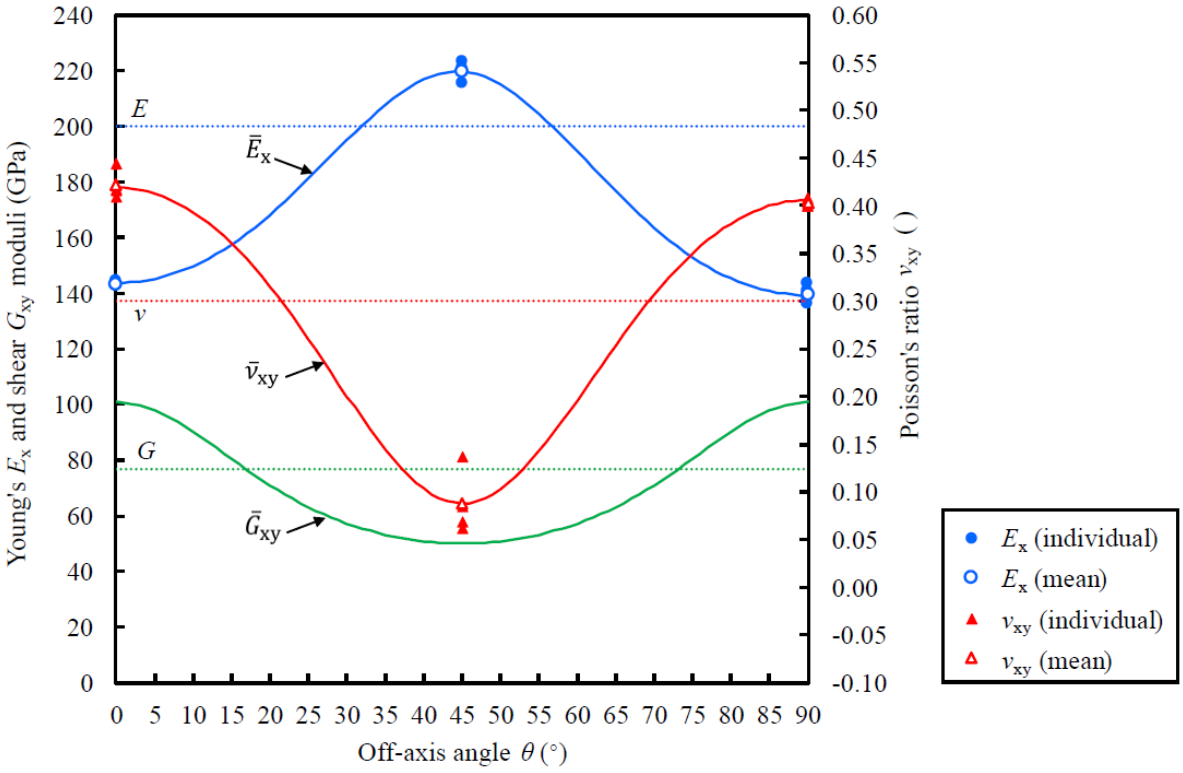

Fig 5: Variation of elastic constants with θ in the machined coupons. The horizontal dotted lines indicate the typical properties of conventionally produced (isotropic) stainless steel. [14]

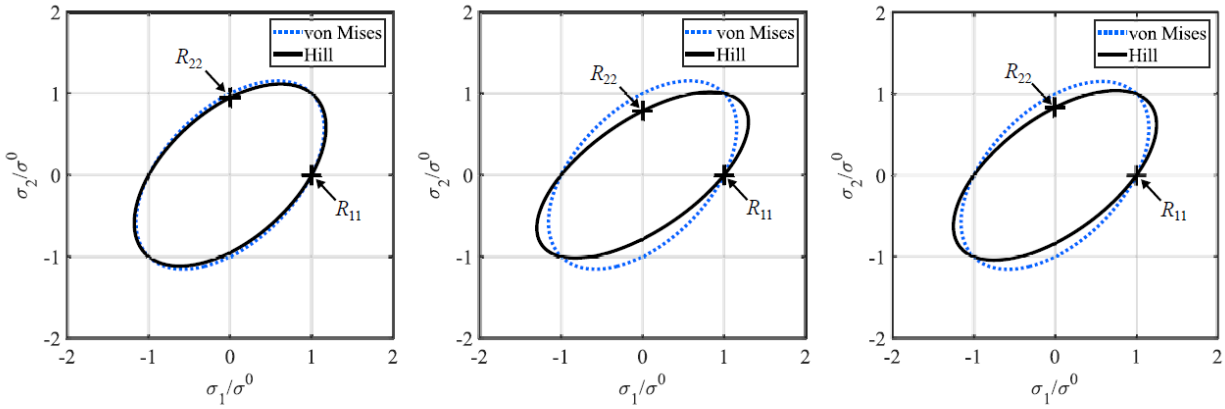

Fig 6: Normalised yield surfaces for the 3 coupon types using the von Mises and Hill yield criteria. [14]

[1] Gao, W.; Zhang, Y.; Ramanujan, D.; Ramani, K.; Chen, Y.; Williams, C.B.; Wang, C.C.L.; Shin, Y.C.; Zhang, S.; Zavattieri, P.D. (2015) *The status, challenges, and future of additive manufacturing in engineering*. Computer Aided Design **69**, 65–89.

[2] Wu, P.; Wang, J.; Wang, X. (2016) *A critical review of the use of 3-D printing in the construction industry*. Automation in Construction **68**, 21–31.

[3] Gardner, L.; Kyvelou, P.; Herbert, G.; Buchanan, C. (2020) *Testing and initial verification of the world's first metal 3D printed bridge.* Journal of Constructional Steel Research **172**, 106233.

[4] Lange, J.; Feucht, T.; Erven, M. (2020) *3D printing with steel: Additive Manufacturing for connections and structures*. Steel Construction **13**, 144–153.

[5] Buchanan, C.; Gardner, L. (2019) *Metal 3D printing in construction: A review of methods, research, applications, opportunities and challenges*. Engineering Structures **180**, 332–348.

[6] Cavazutti, M.; Baldini, A.; Bertocchi, E.; Costi, D.; Torricelli, E. (2011) *High performance automotive chassis design: a topology optimization based approach*. Structural and Multidisciplinary Optimization **44**, 45-56.

[7] Joshi, S.C.; Sheikh, A.A (2015) *3D printing in aerospace and its long-term sustainability*. Virtual and Physical Prototyping **10**, 175-185.

[8] Laghi, V.; Palermo, M.; Tonelli, L.; Gasparini, G.; Ceschini, L.; Trombetti, T. (2020) *Tensile properties and microstructural features of 304L austenitic stainless steel produced by wire-and-arc additive manufacturing*. International Journal of Advanced Manufacturing Technology **106**, 3693–3705.

[9] Wang, L.; Xue, J.; Wang, Q. (2019) *Correlation between arc mode, microstructure, and mechanical properties during wire arc additive manufacturing of 316L stainless steel*. Materials Science and Engineering A **751**, 183–190.

[10] Haghdadi, N.; Laleh, M.; Moyle, M.; Primig, S. (2021) *Additive manufacturing of steels: a review of achievements and challenges*. Journal of Materials Science **56**, 64–107.

[11] Kyvelou, P.; Slack, H.; Mountanou, D.D.; Wadee, A.M.; Britton, T.B.; Buchanan, C.; Gardner, L. (2020) *Mechanical and microstructural testing of wire and arc additively manufactured sheet material*. Materials and Design **192**, 108675.

[12] Luecke, W.E.; Slotwinski, J.A. (2014) *Mechanical properties of austenitic stainless steel made by additive manufacturing*. Journal of Research of the National Institute of Standards and Technology **119**, 398–418.

[13] Hadjipantelis, N.; Weber, B.; Gardner, L. (2021) *Characterisation of the anisotropic response of wire and arc additively manufactured stainless steel.* ce/papers **4**, 1757-1766.
[14] Hadjipantelis, N.; Weber, B.; Buchanan, C.; Gardner, L. (2021) *Description of anisotropic material response of wire and arc additively manufactured thin-walled stainless steel elements*. Thin-walled structures (Accepted).